

High speed photometry of faint cataclysmic variables - VII. Targets selected from the Sloan Digital Sky Survey and the Catalina Real-time Transient Survey

Patrick A. Woudt^{1*}, Brian Warner^{1,2}, Deanne de Budé¹, Sally Macfarlane¹
Matthew P.E. Schurch¹ & Ewald Zietsman¹

¹ *Astrophysics, Cosmology and Gravity Centre, Department of Astronomy, University of Cape Town, Private Bag X3, Rondebosch 7701, South Africa*

² *School of Physics and Astronomy, Southampton University, Highfield, Southampton SO17 1BJ, UK*

Accepted 2011 December 30. Received 2011 December 30; in original form 2011 October 18

ABSTRACT

We present high speed photometric observations of 20 faint cataclysmic variables, selected from the Sloan Digital Sky Survey and Catalina catalogues. Measurements are given of 15 new directly measured orbital periods, including four eclipsing dwarf novae (SDSS0904+03, CSS0826-00, CSS1404-10 and CSS1626-12), two new polars (CSS0810+00 and CSS1503-22) and two dwarf novae with superhumps in quiescence (CSS0322+02 and CSS0826-00). Whilst most of the dwarf novae presented here have periods below 2 h, SDSS0805+07 and SSS0617-36 have relatively long orbital periods of 5.489 and 3.440 h, respectively. The double humped orbital modulations observed in SSS0221-26, CSS0345-01, CSS1300+11 and CSS1443-17 are typical of low mass transfer rate dwarf novae. The white dwarf primary of SDSS0919+08 is confirmed to have non-radial oscillations and quasi-periodic oscillations were observed in the short-period dwarf nova CSS1028-08 during outburst. We further report the detection of a new nova-like variable (SDSS1519+06). The frequency distribution of orbital periods of CVs in the Catalina survey has a high peak near ~ 80 min orbital period, independently confirming that found by Gänsicke et al (2009) from SDSS sources. We also observe a marked correlation between the median in the orbital period distribution and the outburst class, in the sense that dwarf novae with a single observed outburst (over the 5-year baseline of the CRTS coverage) occur predominantly at shortest orbital period.

Key words: techniques: photometric – binaries: close – eclipsing – novae, cataclysmic variables – stars: dwarf novae

1 INTRODUCTION

In six previous papers (references given in Woudt & Warner 2010) we presented results from high speed photometry of faint cataclysmic variables (CVs: see Warner 1995a for a review) that had previously only been poorly studied. We have now observed a further 20 stars, drawn from the Sloan Digital Sky Survey (SDSS: e.g., Abazajian et al. 2009) and the Catalina Real-Time Transient Survey (CRTS: Drake et al. 2009).

The CRTS has detected ~ 650 CVs to date (2011 October) using a network of three telescopes: the 0.7-m Catalina Sky Survey (CSS) Schmidt telescope, the Mt. Lemmon Survey (MLS) 1.5-m Cassegrain and the Siding Springs Survey

(SSS) 0.5-m Schmidt telescope. The CRTS keeps variable objects under surveillance for 21 nights of each lunation, giving good coverage of long-term light curves, and publishes results as they are obtained¹. The CVs detected by the CRTS are largely dwarf novae found from their outbursts - their detection is triggered by outburst amplitudes in excess of 2 mag - and some magnetic CVs (polars) varying between low and high states. Given the depth of the CRTS survey ($V \sim 20.5$ mag), CRTS is able to sample a population of intrinsically faint dwarf novae.

In our high-speed photometric survey we generally sam-

¹ <http://nessi.cacr.caltech.edu/catalina/AllCV.html>

<http://nessi.cacr.caltech.edu/MLS/AllCV.html>

<http://nessi.cacr.caltech.edu/SSS/AllCV.html>

* email: Patrick.Woudt@uct.ac.za

ple CRTS CVs accessible to the Southern African Large Telescope (SALT) in case spectroscopic follow-up is required. This implies that we primarily select CRTS CVs south of declination $+10^\circ$. Within this declination range there are 357 CVs in the CRTS (at 2011 October), of which 241 have been discovered by the CSS telescope, 7 by the MLS telescope (unique identifications, not duplicated in CSS) and 109 have been discovered solely by the SSS telescope.

All of our observations were made with the University of Cape Town (UCT) CCD photometer, as described by O’Donoghue (1995), in frame transfer mode and with white light, on the 1.9-m (74-in) and 1.0-m (40-in) reflectors at the Sutherland site of the South African Astronomical Observatory (SAAO).

In our previous papers, an approximate magnitude scale was derived with the use of hot white dwarf standards (Landolt 1992), but because of the non-standard spectral distributions of CVs and the use of white light, our magnitudes approximate a V scale only to ~ 0.1 mag. Given that our targets in this paper are largely drawn from the SDSS and CRTS surveys, we explored the reliability of using SDSS photometry to calibrate our white light observations. On clear nights when hot white dwarf standards were observed, SDSS stars in the field of view of target CVs revealed a stable zero point offset between V and SDSS r of 0.12 ± 0.05 over a broad range of SDSS $(g-r)$ colour from 0.2 – 1.0. This is consistent with the SDSS r to V photometric transformation described by Jester et al. (2005). The UCT CCD magnitudes quoted in this paper correspond to r photometric system, calibrated by SDSS photometry of stars in the field of view of our targets with $(g-r)$ colours in the range 0.2 – 1.0.

Our work is an ongoing survey – many of the stars reported here will require more intensive and extended study. In Section 2 we give the results of our observations. Section 3 gives brief conclusions.

2 OBSERVATIONS

2.1 SDSS0805+07 (SDSS J080534.49+072029.1)

SDSS0805+07 was announced as a CV in paper VI of the Sloan Digital Sky Survey series (Szkody et al. 2007) where it is listed at magnitude $r = 17.79$ and $(g-r) = 0.73$. The SDSS spectrum contained signs of an early type K absorption spectrum, suggesting that the orbital period would be quite long. The later paper by Gänsicke et al. (2009) on orbital periods of SDSS CVs does not include any further observations of this star.

Our photometric observations of SDSS0805+07 are listed in Tab. 1 and the light curves are shown in Fig. 1. The Fourier transform of the data is shown in Fig. 2 where we have identified the highest peak as twice the orbital frequency (2Ω , where $\Omega = 1/P_{orb}$). We chose this because of the presence of the significant 3Ω signal and a weak Ω signal which shows in the light curve as a slightly larger amplitude for alternate maxima. This choice of orbital period is also driven by the K absorption spectrum mentioned above; the light curve is evidently substantially affected by the ellipsoidal variation of the secondary. The ephemeris for minimum light is

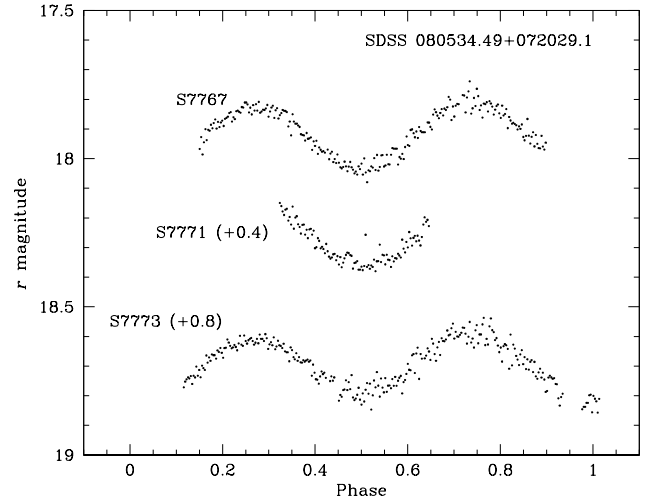


Figure 1. Individual light curves of SDSS 0805, folded on the ephemeris given in Eq. 1. The light curve of S7767 is displayed at the correct brightness. Runs S7771 and S7773 have been displaced vertically by 0.4 and 0.8 mag, respectively.

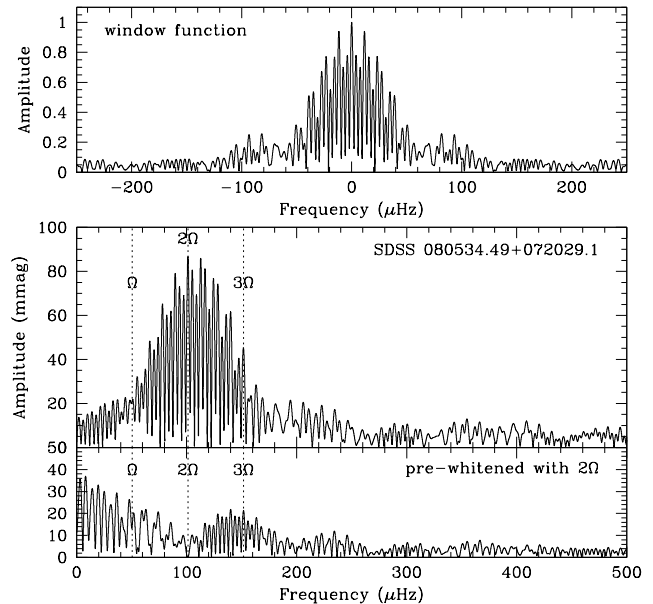


Figure 2. The top panel displays the window function of the FT of the combined runs S7767, S7771 and S7773. The middle panel shows the FT of the combined runs of SDSS 0805 with the orbital frequency (Ω) and its first two harmonics marked by the dashed vertical lines. The lower panel shows the combined FT pre-whitened at the first harmonic (2Ω) of the orbital frequency.

$$\text{HJD}_{\min} = 245\,4464.39 + 0.2287(5) \text{ E.} \quad (1)$$

2.2 SDSS0904+03 (SDSS J090403.49+035501.2)

SDSS0904+03 was listed as a CV in paper III of the SDSS series (Szkody et al. 2004) where it was shown to be a shallow eclipsing system with $P_{orb} = 85.98$ min and prominent white dwarf absorption lines evident in the spectrum. Later photometry by Woudt et al. (2005) showed possible low am-

Table 1. Observing log.

Object	Type	Run No.	Date of obs. (start of night)	HJD of first obs. (+2450000.0)	Length (h)	t_{in} (s)	Tel.	r (mag)
SDSS0805+07	CV	S7767	2007 Dec 29	4464.42448	4.10	60	40-in	17.9
		S7771	2007 Dec 31	4466.52235	1.77	60	40-in	17.9
		S7773	2008 Jan 01	4467.38970	4.92	60	40-in	17.9
SDSS0904+03 eclipsing	CV	S7190	2003 Dec 23	2997.53850	1.53	80	74-in	19.3*
		S7200	2003 Dec 27	3001.49672	2.65	90	74-in	19.4*
		S7216	2003 Dec 31	3005.41754	2.91	45	74-in	19.2*
		S7541	2004 Dec 14	3354.50212	2.29	80	40-in	19.0*
		S7545	2004 Dec 16	3356.50347	2.40	80	40-in	19.0*
		S7600	2005 Mar 08	3438.26907	3.52	100	40-in	19.2*
		S7602	2005 Mar 09	3439.26052	2.53	100	40-in	19.2*
		S7603	2005 Mar 10	3440.26381	2.36	100	40-in	19.2*
		S7604	2005 Mar 11	3441.26385	2.83	100	40-in	19.2*
		S7612	2005 Mar 29	3459.23798	2.12	60	40-in	19.2*
SDSS0919+08	CV	S7212	2003 Dec 30	3004.47499	2.15	30	74-in	18.2:
		S7219	2004 Jan 01	3006.43116	2.29	25	74-in	18.3
		S7235	2004 Feb 09	3045.34260	1.83	100	40-in	18.2
		S7236	2004 Feb 13	3049.36907	0.48	100	40-in	18.1
		S7238	2004 Feb 14	3050.32530	2.80	90	40-in	18.2
		S7243	2004 Feb 15	3051.33939	2.24	100	40-in	18.2
		S7561	2005 Feb 01	3403.44323	2.95	90	40-in	18.3
		S7564	2005 Feb 03	3405.40375	2.55	90	40-in	18.1:
		S7566	2005 Feb 04	3406.39126	4.05	90	40-in	18.3
		S7569	2005 Feb 05	3407.39868	3.47	90	40-in	18.2
		S7572	2005 Feb 06	3408.41099	2.73	90	40-in	18.2
		S7575	2005 Feb 07	3409.40965	1.60	90	40-in	18.2
		S7685	2007 Jan 14	4115.42552	3.83	30	40-in	18.3
		S7687	2007 Jan 15	4116.42147	4.11	30	40-in	18.3
		S7689	2007 Jan 16	4117.43745	2.91	30	40-in	18.2
		S7692	2007 Jan 17	4118.40030	4.93	30	40-in	18.2
		S7695	2007 Jan 18	4119.41123	4.33	30	40-in	18.2
		S7698	2007 Jan 19	4120.42478	4.14	30	40-in	18.2
		S7702	2007 Jan 21	4122.42529	4.27	30	40-in	18.2
		S7705	2007 Jan 22	4123.44064	3.66	30	40-in	18.2
S7707	2007 Jan 23	4124.40915	3.83	30	40-in	18.2		
SDSS1519+06	CV	S7759	2007 Mar 24	4184.54459	2.77	40	40-in	17.1 ^b
		S7762	2007 Mar 26	4186.48546	4.14	40	40-in	17.2 ^b
		S7765	2007 Mar 27	4187.47591	4.11	40	40-in	17.0 ^b
SSS0221-26	DN	S8001	2010 Oct 28	5498.41592	2.34	45	74-in	19.3:
		S8004	2010 Oct 30	5500.33806	4.85	60	74-in	19.3:
		S8006	2010 Oct 31	5501.42365	2.42	60	74-in	19.3:
CSS0332+02	DN	S7881	2009 Dec 16	5182.29440	3.98	90	74-in	20.1
		S7883	2009 Dec 17	5183.28893	3.30	90	74-in	20.1
		S7885	2009 Dec 18	5184.29130	3.13	90	74-in	20.3
		S7889	2009 Dec 20	5186.29202	3.07	90	74-in	20.3
		S7894	2009 Dec 22	5188.35299	1.48	90	74-in	20.0
		S7896	2009 Dec 23	5189.29053	2.85	90	74-in	19.9
CSS0334-07	DN	S7680	2007 Jan 12	4113.28517	1.92	10	40-in	17.8
		S7887	2009 Dec 19	5185.29124	3.18	30	74-in	18.3
		S7996	2010 Sep 19	5458.52966	2.88	95	40-in	18.4
		S8009	2010 Nov 01	5502.42705	4.63	45	74-in	18.6
		S8043	2010 Dec 12	5543.29738	3.80	60	74-in	18.6
CSS0345-01	DN	S8016	2010 Nov 26	5527.29721	4.32	90,100	40-in	18.6:
		S8019	2010 Nov 27	5528.39225	1.70	90	40-in	18.6:
		S8026	2010 Nov 30	5531.34710	5.18	90	40-in	18.7:

Notes: DN = Dwarf Nova; t_{in} is the integration time; * mean magnitude out of eclipse; ‘:’ denotes an uncertain value; ^b observations taken with the SAAO CCD.

Table 1. Continued: Observing log.

Object	Type	Run No.	Date of obs. (start of night)	HJD of first obs. (+2450000.0)	Length (h)	t_{in} (s)	Tel.	r (mag)
SSS0617-36	CV	S8013	2010 Nov 24	5525.39167	2.23	30	40-in	17.6
		S8015	2010 Nov 25	5526.39259	3.45	40,45	40-in	17.7
		S8017	2010 Nov 26	5527.48668	2.52	40	40-in	17.7
		S8020	2010 Nov 27	5528.48484	2.91	30	40-in	17.7
		S8029	2010 Dec 03	5534.35377	5.66	20	40-in	17.9
CSS0810+00	Polar	S7915	2010 Mar 18	5274.25067	4.21	20	74-in	18.1
		S7917	2010 Mar 19	5275.24505	2.81	20	74-in	18.3
		S7923	2010 Mar 21	5277.24549	3.15	20	74-in	18.3
		S7937	2010 Apr 02	5289.25213	2.03	60	40-in	18.2
CSS0826-00 eclipsing	DN	S7892	2009 Dec 21	5187.44515	3.60	90	74-in	20.1*
		S7943	2010 Apr 06	5293.23279	3.49	90	40-in	19.7*
		S7946	2010 Apr 07	5294.22280	3.42	90	40-in	19.9*
		S7957	2010 Apr 11	5298.21867	2.13	90	40-in	19.9*
CSS1028-08	DN	S7918	2010 Mar 19	5275.40553	2.41	6	74-in	16.1
		S7921	2010 Mar 20	5276.38365	3.87	10,15	74-in	17.5
		S7924	2010 Mar 21	5277.39139	4.25	20	74-in	19.0
CSS1300+11	DN	S7971	2010 May 21	5338.31041	3.15	55	74-in	19.9
		S7987	2010 Jun 05	5353.21030	4.14	65	74-in	19.7
		S7989	2010 Jun 06	5354.22694	2.41	65	74-in	19.8
		S7991	2010 Jun 07	5355.21884	2.22	65	74-in	19.6
CSS1321+01 = HV Vir	DN	S7935	2010 Apr 01	5288.43811	3.39	100	40-in	19.4
		S7939	2010 Apr 02	5289.48174	3.45	100	40-in	19.5
		S7944	2010 Apr 06	5293.38817	4.17	100	40-in	19.5
		S7947	2010 Apr 07	5294.37465	4.47	100	40-in	19.4
		S7950	2010 Apr 08	5295.37400	1.61	100	40-in	19.5
CSS1404-10 eclipsing	DN	S7833	2009 Feb 27	4890.58682	1.00	60	74-in	19.6*
		S7848	2009 Mar 20	4911.45607	3.75	15	74-in	16.6*
		S7851	2009 Mar 21	4912.46066	4.76	15	74-in	17.3*
		S7853	2009 Mar 22	4913.43818	2.15	30	74-in	18.4*
		S7858	2009 Mar 23	4914.48481	4.16	30	74-in	18.8*
		S7862	2009 Jun 12	4995.21939	2.63	45	74-in	19.4*
CSS1443-17	DN	S7865	2009 Jun 17	5000.19997	4.28	60	74-in	19.1
		S7869	2009 Jun 18	5001.20840	3.50	60	74-in	19.1
CSS1503-22	Polar	S7925	2010 Mar 21	5277.58370	1.78	90	74-in	17.2
		S7929	2010 Mar 22	5278.60089	1.57	55	74-in	17.2
		S7931	2010 Mar 23	5279.52952	3.01	20	74-in	17.5
		S7962	2010 Apr 12	5299.48901	4.05	30	40-in	17.2
		S7965	2010 Apr 13	5300.45963	4.50	30	40-in	17.3
CSS1528+03	DN	S7940	2010 Apr 02	5289.63048	0.60	20	40-in	17.0
		S7956	2010 Apr 10	5297.45581	4.40	90	40-in	19.5
		S7959	2010 Apr 11	5298.41794	5.73	90	40-in	19.3
		S7961	2010 Apr 12	5299.41131	1.70	90	40-in	19.9
CSS1626-12 eclipsing	DN	S7985	2010 Jun 04	5352.40913	4.43	90	74-in	20.4*
		S7988	2010 Jun 05	5353.40403	3.95	90	74-in	20.3*
		S7990	2010 Jun 06	5354.41289	3.05	90	74-in	20.4*
CSS2325-08 = EG Aqr	DN	S7814	2008 Oct 15	4755.26078	1.90	60	74-in	19.3:
		S7815	2008 Oct 16	4756.25083	4.58	30	74-in	19.3:
		S7817	2008 Oct 17	4757.24637	5.50	60	74-in	19.3:
		S7819	2008 Oct 18	4758.24330	6.31	60	74-in	19.2:
		S7821	2008 Oct 19	4759.25972	4.02	60	74-in	19.3:
		S7824	2008 Oct 20	4760.38167	1.22	60	74-in	19.4:

Notes: DN = Dwarf Nova; t_{in} is the integration time; * mean magnitude out of eclipse; ':' denotes an uncertain value.

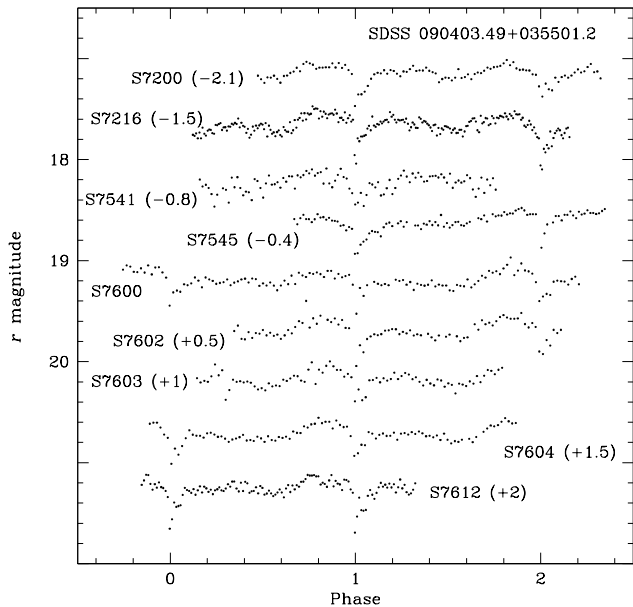


Figure 3. Individual light curves of SDSS 0904, folded on the ephemeris given in Eq. 2. The light curve of S7600 is displayed at the correct brightness; vertical offsets for each light curve are given in brackets.

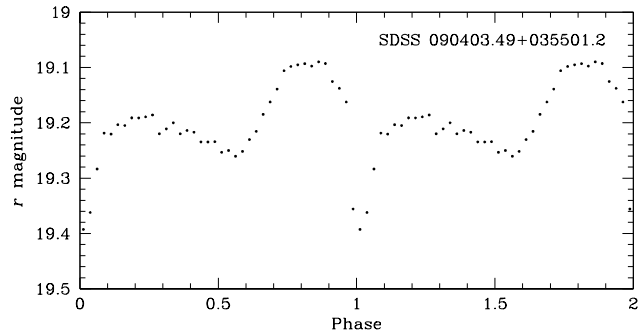


Figure 4. The average light curve of SDSS 0904 during March 2005, folded on the ephemeris given in Eq. 2.

plitude (24 mmag) variations with a period ~ 740 s, classifying it as a candidate CV/ZZ star - i.e. a CV containing a nonradially pulsating white dwarf (a ZZ Cet star). Our observations are listed in Tab. 1, the individual light curves are shown in Fig. 3 and an average light curve for the March 2005 runs is shown in Fig. 4, which is typical of a low mass transfer dwarf nova. An FT of the whole data set provides $P_{orb} = 86.0015$ min and the eclipse ephemeris

$$\text{HJD}_{\min} = 245\,3438.2843 + 0.05972325 (2) \text{ E.} \quad (2)$$

There are no significant peaks in the FTs at higher frequencies in our larger data set, so SDSS0904+03 appears not to be a pulsating system. We now think that the earlier tentative detection of power at 740 s was caused by a high harmonic of the eclipse profile.

2.3 SDSS0919+08 (SDSS J091945.11+085710.0)

SDSS0919+08 was recognised as a CV in paper IV of the SDSS series (Szkody et al. 2005), where it is given as magni-

tude $g = 18.20$. The spectrum shows Balmer emission with underlying absorption spectrum of a white dwarf. From a small number of spectra an orbital period of 84 ± 8 min was deduced. Mukadam et al. (2007) detected a periodic signal in the light curve which gave 91 ± 7 min for P_{orb} and found a further low amplitude ($\sim 1\%$) brightness modulation near 260 s in 5 out of 6 light curves, which might be a doublet with splitting ~ 1.3 s. They estimated an effective temperature of 13 000 K for the white dwarf. The nature of the 260 s periodicity was not ascertained - it could be a rotationally or magnetically split nonradial oscillation, or directly related to a spin period.

Dillon et al. (2008) found an orbital period of 81.6 ± 1.2 min from a 3 h high speed photometry run on one night with the Calar Alto 2.2-m reflector, and Szkody et al. (2010) found a possible P_{orb} harmonic at 40.75 min with the Hubble Space Telescope but no high frequency modulation at all with various ground based telescopes in 2007/2008. Their conclusion was that SDSS0919+08 had at least temporarily stopped pulsating.

Our photometric runs on SDSS0919+08 are listed in Tab. 1; they were made mostly in 2004 February, 2005 February and 2007 January. The FTs are shown in Fig. 5. We saw no modulation above 5% in 2004 and none above 3% in 2007 (in agreement with Szkody et al. observations described above) but in 2005 February there was not only a $\sim 8\%$ modulation at 260 s but also a 6% amplitude at 214 s. The first of these is a $\sim 3\sigma$ spike and is at the period often seen before, so there is no doubt about its reality. For the shorter period oscillation we show in Fig. 6 an amplitude (A) - phase (ϕ) diagram for runs S7561, S7564 and S7572, respectively, obtained in 2005 February. These illustrate the high coherence of the 214-s oscillation (f_2) with a drift in frequency that is commonly seen in oscillation white dwarfs with unresolved multiplets.

The presence of two simultaneous frequencies excludes a simple white dwarf rotation model for SDSS J0919+08, but is indicative of nonradial oscillations in the white dwarf.

2.4 SDSS1519+06 (SDSS J151915.86+064529.1)

SDSS1519+06 is another object in the Sloan data base, listed at $r = 16.74$ and $(g - r) = -0.17$, which has colours similar to that of CVs. We observed it on three nights in 2007 March (see Tab. 1) using the SAAO CCD; the light curves are displayed in Fig. 7 and show very active flickering characteristic of a CV but no periodic modulations.

Since making these observations an SDSS spectrum is available on the SDSS Skyserver which shows a strong blue continuum, narrow Balmer emission lines and a strong He II emission which are characteristic of a low inclination nova-like variable.

2.5 SSS0221-26 (SSS100511:022138-261952)

SSS0221-26 is a Catalina source (100511:022138-261952) discovered at the Siding Spring Observatory in Australia. We observed it on three nights as listed in Tab. 1 and the light curves are shown in Fig. 8.

The FT shows maximum power at the fundamental and first harmonic of a 101.5-min periodicity, but the 1-d alias

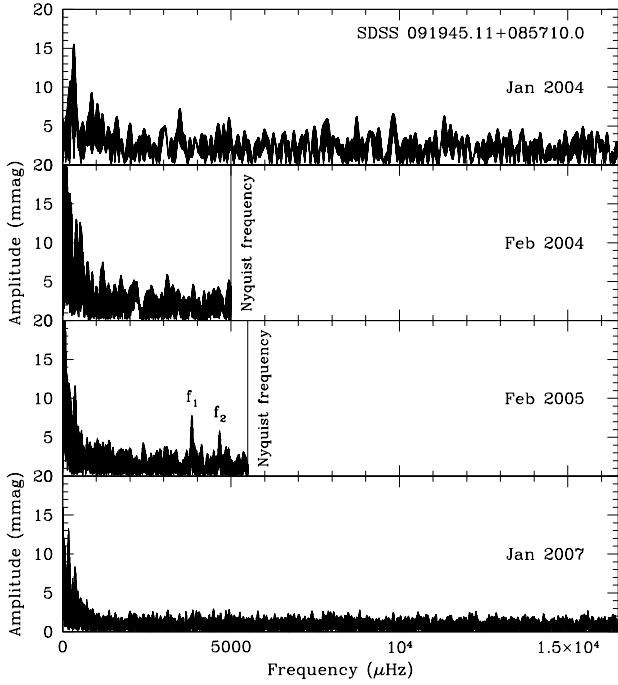


Figure 5. The combined FTs of SDSS 0919 during 2004 January, February, 2005 February and 2007 January, respectively.

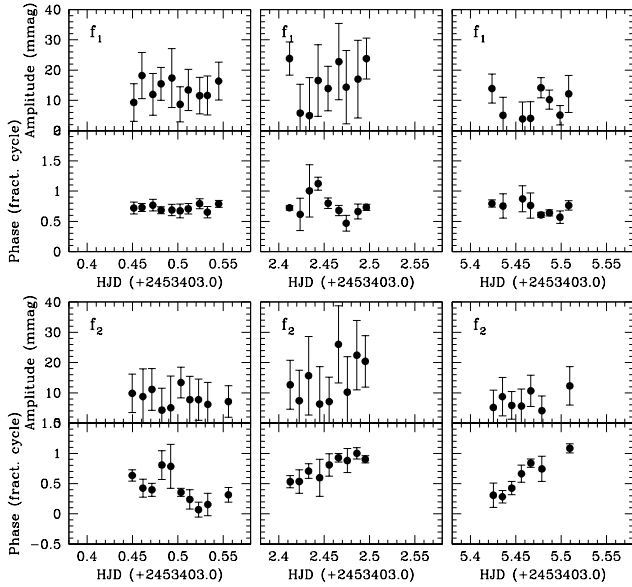


Figure 6. The phase (ϕ) and amplitude (A) diagrams for f_1 (upper two rows) and f_2 (bottom two rows) of SDSS0919 on three different nights in 2005 February. Each dot represents ~ 5 cycles of the 260-s modulation (f_1) or ~ 6 cycles of the 214-s modulation (f_2), with a 33% overlap. In the phase diagrams, only those points are plotted where the amplitude of the modulation is larger than 3 mmag.

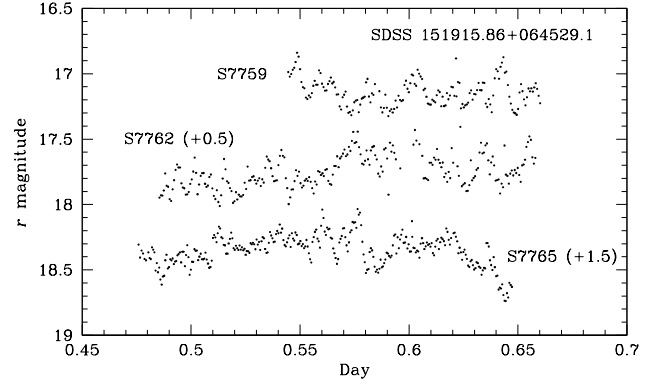


Figure 7. Individual light curves of SDSS 1519+06. The light curve of run S7759 is displayed at the correct brightness; vertical offsets of each light curve are given in brackets.

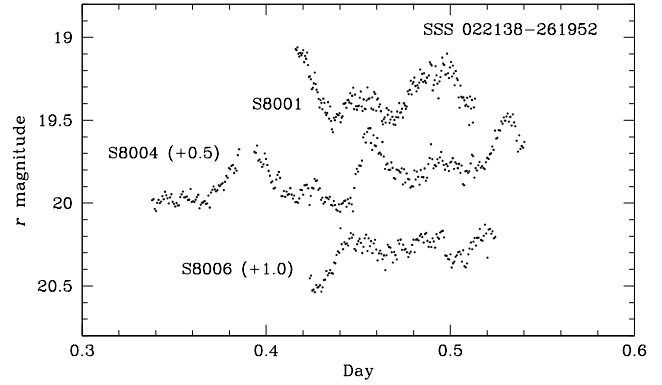


Figure 8. Individual light curves of SSS0221-26. The light curve of run S8001 is displayed at the correct brightness; vertical offsets of each light curve are given in brackets.

at 109.1 min cannot be excluded. The mean light curve at 101.5 min is shown in Fig. 9 which is again characteristic of a low mass transfer dwarf nova in quiescence. The ephemeris for maximum light is:

$$\text{HJD}_{\text{max}} = 245\,5458.4170 + 0.07049(9) \text{ E.} \quad (3)$$

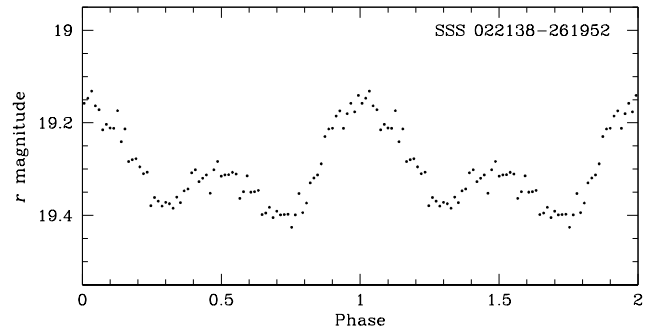


Figure 9. The average light curve of SSS0221-26, folded on the ephemeris given in Eq. 3.

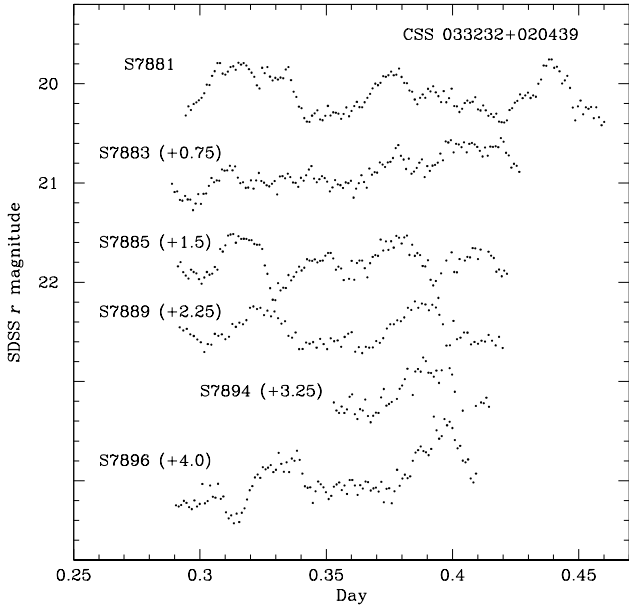


Figure 10. Individual light curves of CSS0332+02. The light curve of run S7881 is displayed at the correct brightness; vertical offsets of each light curve are given in brackets.

2.6 CSS0332+02 (CSS091121:033232+020439)

CSS0332+02 is a Catalina source (091121:033232+020439) that has had three known outbursts, reaching $V \sim 17$, in 2006 October, 2007 October and 2009 November. At quiescence it is fainter than $V \sim 20$ in the Catalina light curve. Our observations are listed in Tab. 1 and were obtained less than a month after the last recorded outburst, when CSS0332+02 was at $r \sim 20.1$. The light curves are shown in Fig. 10 and exhibit profiles typical of orbital or superhump modulations. They turn out to be a combination of both. The FT of the full data set is shown in the upper left panel of Fig. 11 - with the window pattern next to it. The highest peak in the alias pattern in the FT is marked f_{sh+} and its first harmonic is marked $2f_{sh+}$; these are the only two components of the two patterns that have a 2:1 frequency ratio within the small errors involved ($\sim 1\mu\text{Hz}$). Pre-whitening with these two frequencies leaves the FT shown in the lower panel of Fig. 11 - revealing a further alias pattern (which was easily seen in the original total FT), where we have marked the maximum component f_{sh-} . In addition there is a very low amplitude residual alias pattern labelled 2Ω . The frequencies are given in Tab. 2.

With this choice the implied value of the orbital frequency $\Omega = 189.1 \mu\text{Hz}$ is roughly midway between the frequencies f_{sh+} and f_{sh-} , which we claim are positive and negative superhumps. Note that the positive superhump excess $\epsilon^+ = (P_{sh+}/P_{orb}) - 1 = 0.0231$ and the negative superhump deficiency $\epsilon^- = (P_{sh-}/P_{orb}) - 1 = -0.0204$ are close to values for an SU UMa type dwarf nova with $P_{orb} \sim 88.14$ min (Patterson et al. 2005). Note also that the largest modulation is the positive superhump, and its strong first harmonic is typical of the non-sinusoidality of such superhumps.

Our interpretation of this data set is that CSS0332+02 is a dwarf nova showing both positive and negative superhumps (and the first harmonic of P_{orb}) in quiescence. We

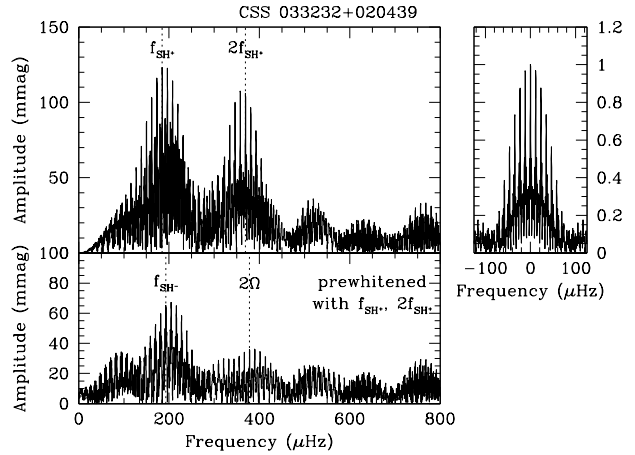


Figure 11. The Fourier transform of CSS0332+02 for the complete data set (top panel: left); the mean and trend has been removed for each individual run. The window function is shown in the top right panel. The lower panel shows the Fourier transform pre-whitened at the negative superhump frequency and its first harmonic. Frequencies listed in Tab. 2 have been marked by dashed vertical lines and labelled.

Table 2. Frequencies observed in CSS0332+02.

ID	Frequency (μHz)	Period (h)	Ampl. (mag)
f_{sh+}	184.81 ± 0.03	1.503	0.119 ± 0.006
$2f_{sh+}$	369.27 ± 0.04	0.752	0.104 ± 0.006
f_{sh-}	193.08 ± 0.05	1.439	0.067 ± 0.005
2Ω	378.23 ± 0.11	0.734	0.036 ± 0.005

arrived at this surprising conclusion partly with the help of the work of Olech, Rutkowski & Schwarzenberg-Czerny (2009) who found that SDSS2100+00 has persistent negative superhumps in quiescence, and moreover was the third such dwarf nova “bihumper” to be found, the others being V503 Cyg (Harvey et al. 1995) and BF Ara (Olech, Rutkowski & Schwarzenberg-Czerny 2007). But in SDSS2100+00, V503 Cyg and BF Ara the positive superhumps are only seen during superoutbursts. The uniqueness of this interpretation encourages further extensive observations.

2.7 CSS0334-07 (CSS091027:033450-071048)

CSS0334-07 is CSS091027:033450-071048 with a quiescent magnitude $V \sim 18.5$; the Catalina light curve shows outbursts to $V \sim 15$ on a time scale of ~ 200 d. This star is also listed in the Sloan Survey as SDSS J033449.87-071047.8 (Szkody et al. 2007), identified as a dwarf nova with $g = 14.64$ (caught by SDSS in outburst) with a candidate orbital period of somewhat less than 2 hours derived from spectroscopy. Kato (2009) reported a superhump period of 107.8 min.

Our observations are listed in Tab. 1; the light curves seen in Fig. 12 possess typical flickering with a range of ~ 0.5 mag, but no modulation on time scales of the proposed orbital period.

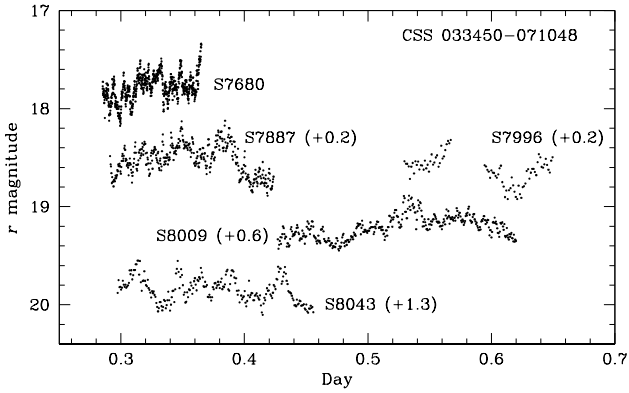


Figure 12. Individual light curves of CSS0334-07. The light curve of run S7680 is displayed at the correct brightness; vertical offsets for each light curve are given in brackets.

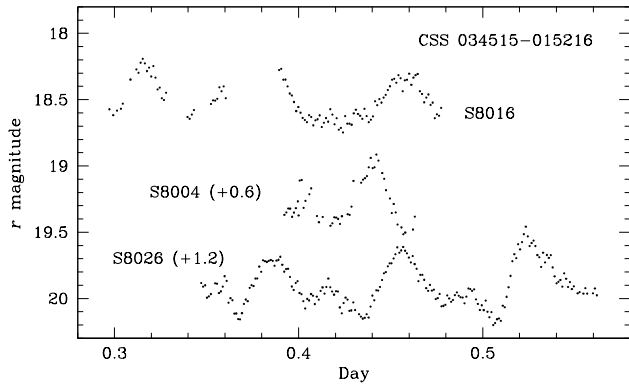


Figure 13. Individual light curves of CSS0345-01. The light curve of run S8016 is displayed at the correct brightness; vertical offsets for each light curve are given in brackets.

2.8 CSS0345-01 (CSS090219:034515-015216)

CSS0345-01 was first reported in the CSS survey in 2009 February as CSS090219:034515-015216. It has a quiescent magnitude around $V \sim 19$ and has had seven recorded outbursts since 2005, reaching up to $V \sim 15.7$.

We observed CSS0345-01 during quiescence in 2010 November (see Tab. 1) when it was around $r \sim 18.6$. The light curves are shown in Fig. 13 and resemble those of SSS0221-26, characteristic of a low mass transfer dwarf nova. The FT of the combined observing runs (Fig. 14) reveals two distinct peaks at $164.81 \pm 0.04 \mu\text{Hz}$ and $330.01 \pm 0.05 \mu\text{Hz}$, which we assign as the fundamental and first harmonic, respectively, of the orbital frequency. The average light curve of CSS0345-01, folded on the orbital period of 101.1 min, is shown in Fig. 15. The ephemeris for maximum light is:

$$\text{HJD}_{\text{max}} = 245\,5527.31408 + 0.07018 (4) \text{ E.} \quad (4)$$

2.9 SSS0617-36 (SSS100511:061754-362655)

SSS100511:061754-362655 (SSS0617-36 hereafter) was first reported by the SSS survey in 2010 May. It has regular outbursts reaching outburst amplitudes of up to 4 magnitude, varying from $V \sim 18$ to ~ 14.2 .

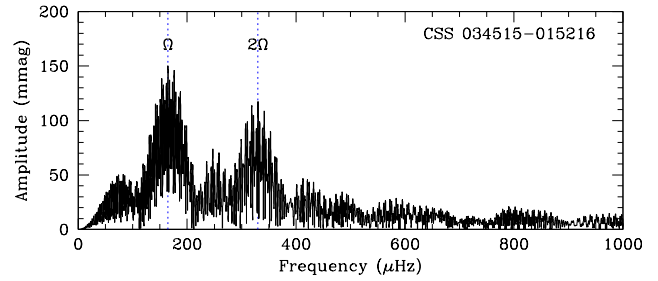


Figure 14. Fourier transform of CSS0345-01 during 2010 November. The orbital frequency (Ω) and its first harmonic (2Ω) are labelled and marked by vertical dashed lines.

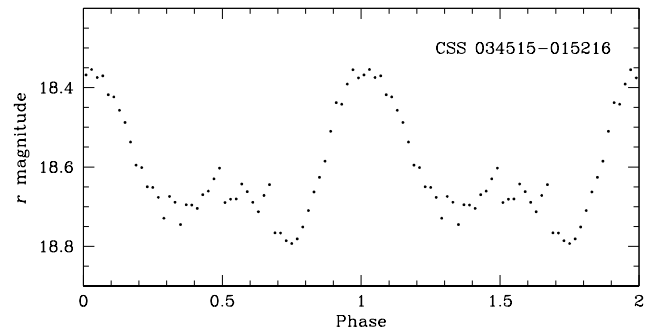


Figure 15. The average light curve of CSS0345-01, folded on the ephemeris given in Eq. 4.

We observed SSS0617-36 during quiescence in 2010 November when the system averaged around $r \sim 17.7$. The light curves are shown in Fig. 16. The light curves are characterised by a large-amplitude orbital modulation (by about a factor of 2 in brightness) and low-amplitude flickering. The orbital modulation, clearly shown in the average light curve (Fig. 17), is non-sinusoidal with power in the Fourier transform at the fundamental frequency ($80.72 \mu\text{Hz}$) and the first two harmonics ($161.53 \mu\text{Hz}$ and $242.20 \mu\text{Hz}$, respectively). The light curve is unusual for a CV and at this stage we cannot provide a specific class. The orbital ephemeris for maximum light is

$$\text{HJD}_{\text{max}} = 245\,5525.46712 + 0.14335 (5) \text{ E.} \quad (5)$$

2.10 CSS0810+00 (CSS100108:081031+002429)

CSS0810+00 is CSS100108:081031+002429; its long-term light curve shows brightness variations from $V \sim 21$ to $V \sim 17.3$ on a range of time scales (Fig. 18, data kindly provided by Dr. Andrew Drake). From that light curve alone it would be difficult to state what kind of CV this is. Our observations are listed in Tab. 1 and the light curves are given in Fig. 19 and were obtained during a high state of CSS0810+00. There are deep minima with depths ~ 1.5 mag and irregular profiles recurring with period 116.15 min. The light curve is very similar to that of the polar V834 Cen in the V band which also has ~ 2 mag range around the orbit (Sambruno et al. 1991). This is compatible with the long term light curve shown in Fig. 18. The ephemeris for minimum light is

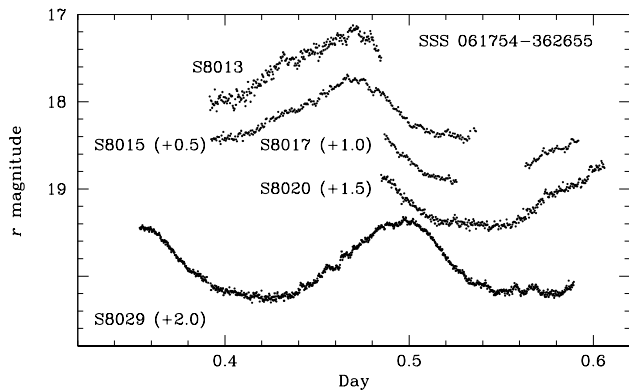


Figure 16. Individual light curves of SSS0617-36. The light curve of run S8013 is displayed at the correct brightness; vertical offsets of each light curve are given in brackets.

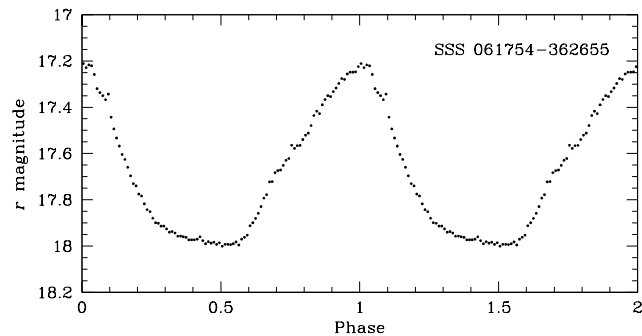


Figure 17. The average light curve of SSS0617-36, folded on the ephemeris given in Eq. 5.

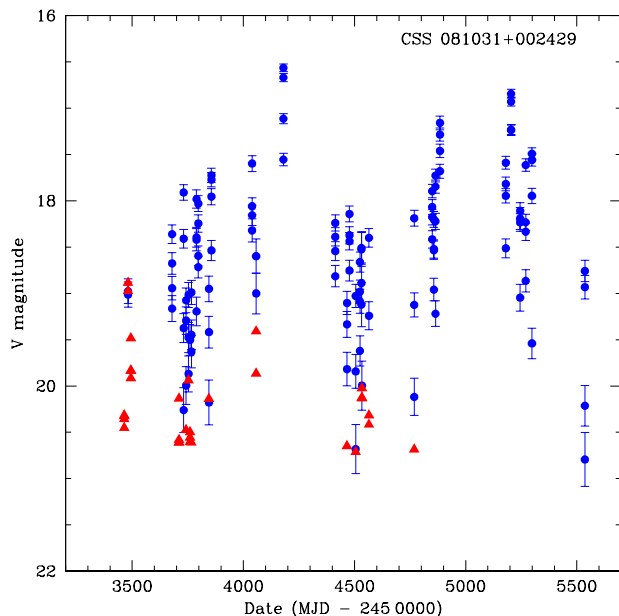


Figure 18. The long term CSS light curve of CSS0810+00. The filled triangles represent upper limits; times are given in heliocentric modified Julian date.

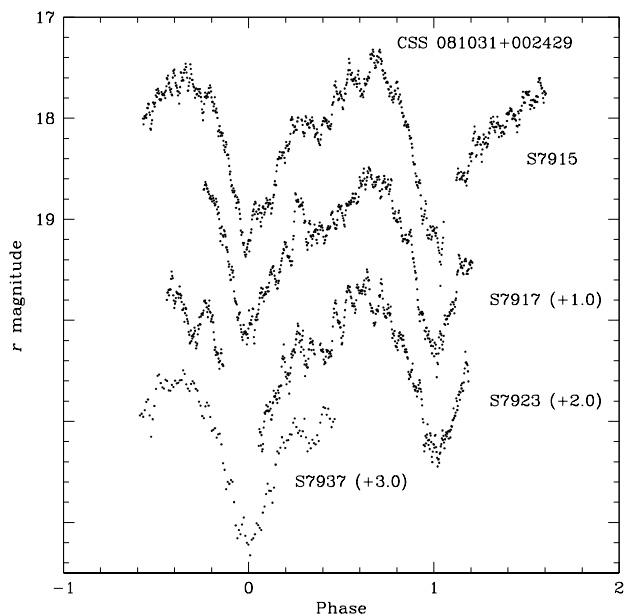


Figure 19. Individual light curves of CSS0810+00, folded on the ephemeris given in Eq. 6. The light curve of run S7915 is displayed at the correct brightness; vertical offsets for each light curve are given in brackets.

$$\text{HJD}_{\min} = 245\,5274.2967 + 0.080660 (2) \text{ E.} \quad (6)$$

2.11 CSS0826-00 (CSS080306:082655-000733)

CSS0826-00 is CSS080306:082655-000733 and has had two observed outbursts raising it from quiescent magnitude $r \sim 20$ to 16.3 and 17.7 respectively. Our observations were made at quiescence with $r = 19.9$ and are listed in Tab. 1. The light curves, displayed in Fig. 20, show that CSS0826-00 is an eclipsing system, descending to $r \sim 21.0$ at mid-eclipse with $P_{\text{orb}} = 86.05$ min. The eclipse ephemeris is

$$\text{HJD}_{\min} = 245\,5293.3415 + 0.05976 (1) \text{ E.} \quad (7)$$

Signs of a superhump drifting through the light curve can be seen in Fig. 20, and the FT confirms this, giving a negative superhump period of 83.63 min; the superhump ephemeris is

$$\text{HJD}_{\text{SH,max}} = 245\,5293.2379 + 0.05807 (3) \text{ E.} \quad (8)$$

The nightly-averaged light curves folded on the superhump ephemeris are shown in Fig. 21. Thus CSS 0826-00 is another SU UMa type dwarf nova with negative superhumps persisting in quiescence, with a negative superhump deficiency of $\epsilon^- = -0.0279$.

2.12 CSS1028-08 (CSS090331:102843-081927)

CSS1028-08 is CSS 090331:102843-081927 which in the CSS light curve has outbursts at intervals as short as 300 d, but with frequent short-lived dips to $V > 20.5$. Our observations are listed in Tab. 1 and the light curves are shown in Fig. 22. CSS1028-08 was descending to quiescence from an outburst (which was missed in the Catalina survey). We do not see any excursions to faint magnitudes in quiescence, and are

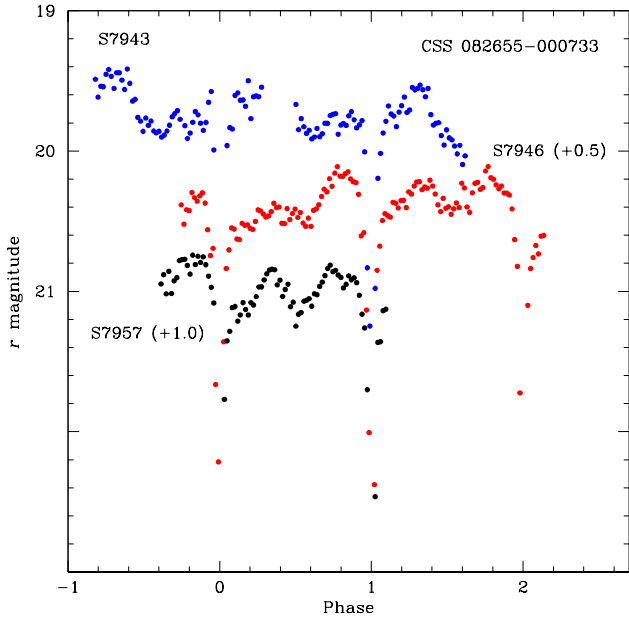


Figure 20. Individual light curves of CSS0826-00, folded on the ephemeris given in Eq. 7. The light curve of run S7943 is displayed at the correct brightness; vertical offsets for each light curve are given in brackets.

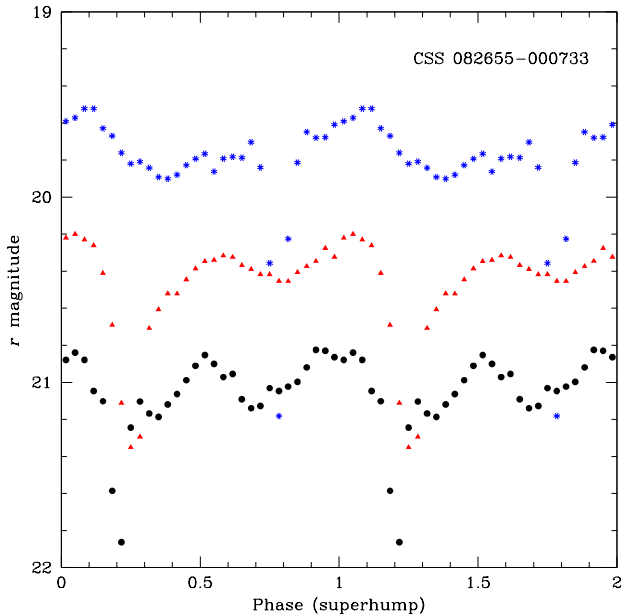


Figure 21. Nightly-averaged light curves of CSS0826-00, folded on the negative superhump ephemeris given in Eq. 8. The light curve of run S7943 is displayed at the correct brightness. Runs S7946 and S7957 have been displaced vertically by 0.5 and 1.0 mag, respectively.

unable to ascertain the cause of the ones in the CSS light curve and suspect that because the star has a close companion the CSS photometry has difficulty in resolving the two. In our photometry the two stars are completely resolved.

CSS1028-08 was observed during superoutburst by Kato et al (2009), who named it OT J1028 and found a

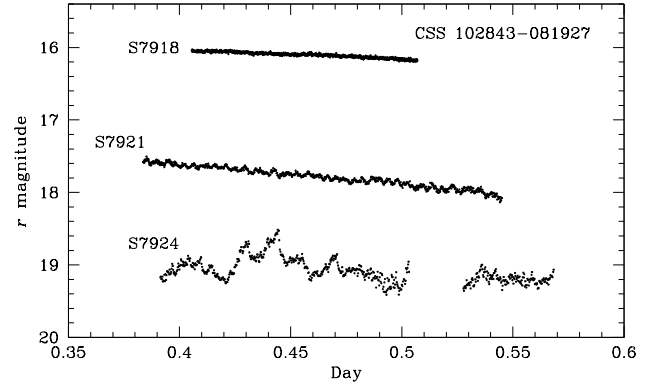


Figure 22. Individual light curves of CSS1028-08. All the light curves are displayed at their correct brightness.

superhump period of 54.85 min, which puts it in the rare class of ultra-short period CVs, similar to V485 Cen and EI Psc, probably with a lowered H/He abundance ratios. The absence of superhumps in run S7918 suggests we observed CSS1028-08 during a normal outburst.

The FTs of runs S7918 and S7921 are shown in Fig. 23. The highest peak in the FT of run S7921 is at 52.1 ± 0.6 min, which we identify as the orbital period; this gives a positive superhump excess of $\epsilon^+ = 0.0530$. The FT of run S7918 shows two short-period modulations which are at 312 s and 86.9 s, which we interpret respectively as a quasi-periodic oscillation (QPO) and a longer-period dwarf nova oscillation of the kinds frequently seen in outbursting dwarf novae (Warner 2004). A similar peak at 345 s is seen in the FT of run S7921, with a lot of additional power at nearby frequencies. The reason for the complexity of the FT is seen in the phase - amplitude diagram shown in Fig. 24; it is clear that there is a persistent oscillation which both drifts and jumps in frequency, again typical of such rapid oscillations. Of particular interest is the phase change seen in Fig. 24 between HJD 245 5276.45 and 245 5276.50 where the QPO period changed from 387 s to 345 s; their frequency difference is approximately equal to the orbital frequency and suggests a temporary change from a sidereal to a synodic (reprocessed) QPO signal.

2.13 CSS1300+11 (CSS080702:130030+115101)

CSS1300+11, is CSS080702:130030+115101 and shows a superoutburst in the CSS long-term light curve, reaching $V = 13.9$ in 2008 July from a quiescent level of $V \sim 20$. It was observed by Kato et al (2009) who measured a superhump period of 92.72 min. We observed it in 2010 June to find the orbital period. Our observations are listed in Tab. 1 and the average light curve is shown in Fig. 25. The orbital period is 90.24 min, which gives a fractional superhump period excess of $\epsilon^+ = 0.0274$; this is in agreement with the general correlation between ϵ^+ and P_{orb} (Patterson et al. 2003). The orbital ephemeris for the time of maximum brightness is

$$\text{HJD}_{\text{max}} = 245\,5338.3346 + 0.06267(1) \text{ E.} \quad (9)$$

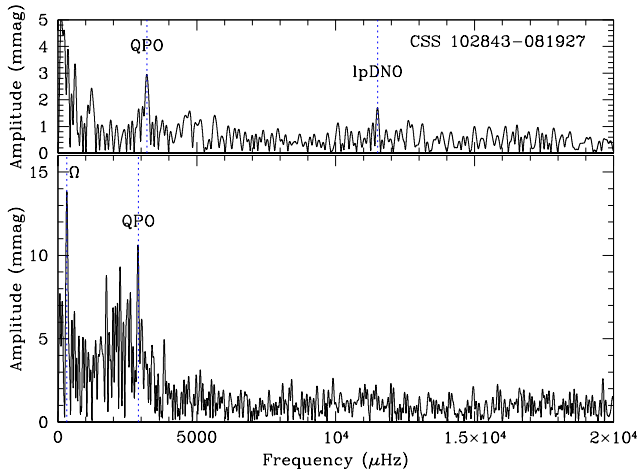


Figure 23. Fourier transforms of CSS1028-08; run S7918 is displayed in the upper panel, run S7921 is shown in the lower panel. Quasi-periodic and longer-period dwarf nova oscillations are marked and labelled. The orbital modulation (Ω) is marked in the lower panel.

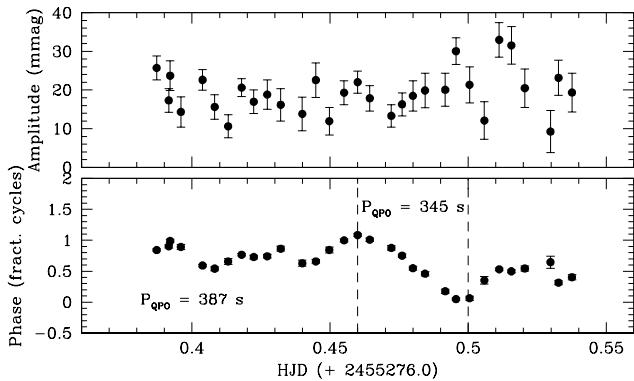


Figure 24. The phase - amplitude diagram for run S7921 of CSS1028-08, relative to the QPO period of 387 s. Between the vertical dashed lines the phase shift indicates the period had changed to 345 s.

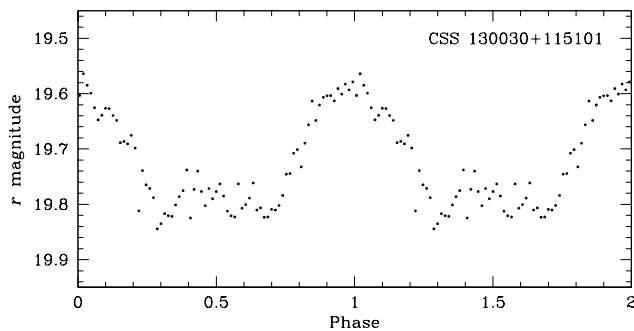


Figure 25. The average light curve of CSS1300+11, folded on the ephemeris given in Eq. 9.

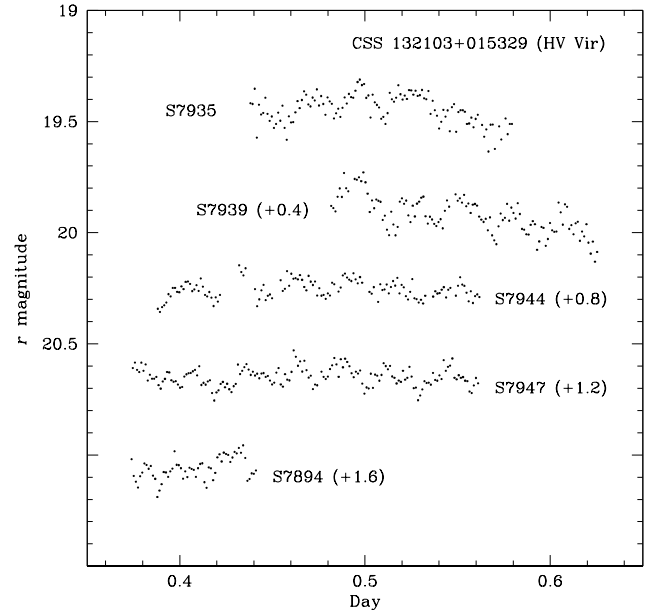


Figure 26. Individual light curves of CSS1321+01. The light curve of run S7935 is displayed at the correct brightness; vertical offsets for each light curves are given in brackets.

2.14 HV Vir (CSS080227:132103+015329)

CSS1321+01 = HV Vir, is CSS 080227:132103+015329, had a superoutburst in 2002 January after a decade of quiescence, reaching $V = 14.15$ in the CSS light curve, from a general quiescent level of $V \sim 19.2$. This star has been well observed during supermaxima, so its superhump period is well determined at 83.82 min, but the observations at quiescence by Patterson et al. (2003) showed two periodicities in the FT: a double humped definite one at $P = 82.18$ min which is P_{orb} and another, less certain at 128.6 min or its alias at 117.9 min.

We observed HV Vir in quiescence in 2010 April; our observations are listed in Tab. 1 and the light curves are shown in Fig. 26. The FT of these light curves, shown in Fig. 27, contains a strong signal at the first harmonic of the orbital frequency (i.e. at 2Ω) and a detectable signal at Ω itself; but in addition there is a window pattern at lower frequency, stronger than the Ω modulation, with period 126.0 min or 117.4 min. Within the uncertainties these are identical to the signal and its alias observed by Patterson et al. These independent data sets confirm the existence of a luminosity modulation at ~ 127 min or its alias at 117 min, the origin of which is not known.

2.15 CSS1404-10 (CSS080623:140454-102702)

CSS1404-10, CSS080623:140454-102702) has a quiescent brightness level of $V \sim 19.5$ in the CSS light curve, with an outburst to $V \sim 15.0$ and others to $V \sim 16.5$ at intervals of ~ 500 d. Our observations were made at quiescence in 2009 February and June, and during the decline of a superoutburst in 2009 March: they are listed in Tab. 1. The light curves are displayed in Fig. 28 and show narrow eclipses more than one magnitude deep in quiescence. The orbital period is 85.794 min and the eclipse ephemeris is

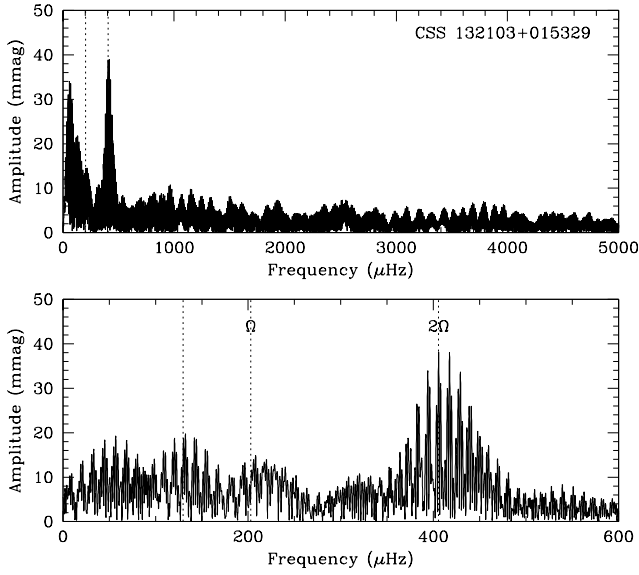


Figure 27. Fourier transform of CSS1321+01 during 2010 April. The orbital frequency (Ω) and its first harmonic (2Ω) are labelled and marked by vertical dashed lines. The 127-min (or 117-min) modulation of unknown origin is also marked by a vertical dashed line.

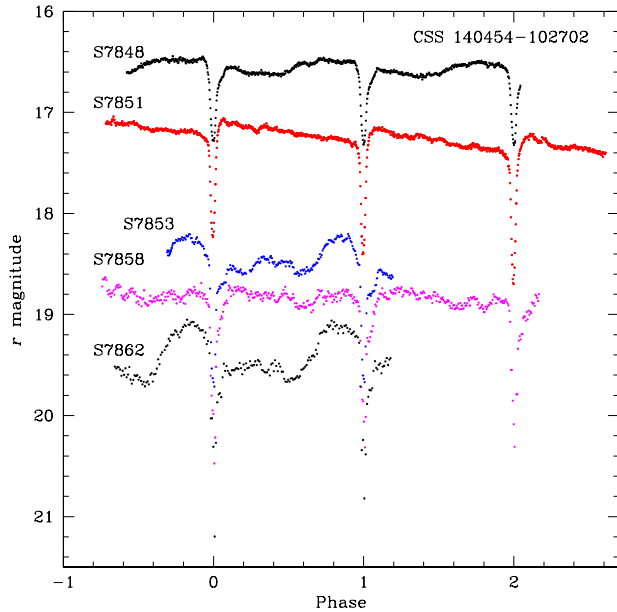


Figure 28. Individual light curves of CSS1404-10, folded on the ephemeris given in Eq. 10. All light curves are displayed at their correct brightness.

$$\text{HJD}_{\min} = 245\,4911.49044 + 0.0595790 (2) \text{ E.} \quad (10)$$

Superhumps were evident during the superoutburst. Their period is 87.81 min, with a resultant superhump period excess of $\epsilon^+ = 0.0238$. The average superhump light curve, folded on the superhump period and with the orbital eclipses excised, showing the typical saw-tooth shape, is given in Fig. 29.

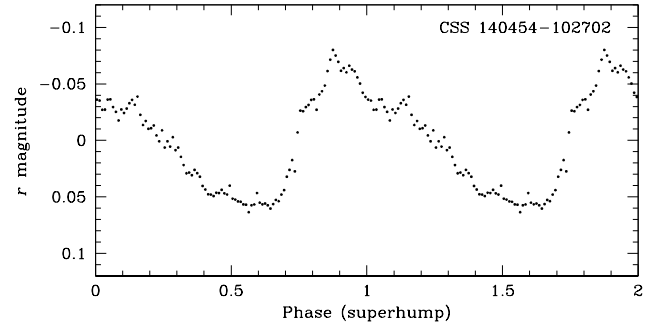


Figure 29. The average light curve of CSS1404 during superoutburst (runs S7848, S7851; eclipses removed), folded on the superhump period of 0.06098 d.

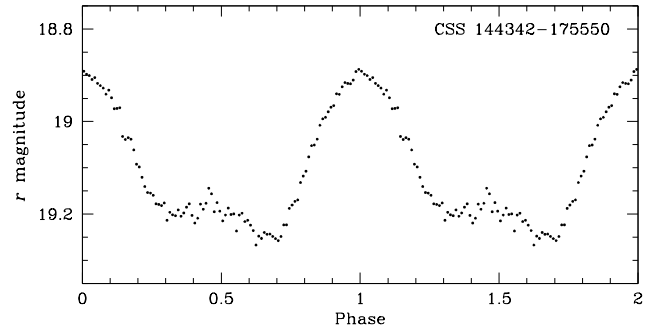


Figure 30. The average light curve of CSS1443-17, folded on the ephemeris given in Eq. 11.

2.16 CSS1443-17 (CSS090418:144342-175550)

CSS1443-17, or CSS 090418:144342-175550, has one superoutburst in the CSS light curve, in 2009 April, which was observed by Kato et al (2009), where it is listed as OT J1443, and who found superhumps with a period of 103.77 min. We observed it at quiescence in 2009 June - the observations are listed in Tab. 1 - and found it to have a strong orbital modulation with a range of 0.3 mag, as seen in the average light curve in Fig. 30. The orbital period is 101.1 min and the ephemeris for maximum light is

$$\text{HJD}_{\max} = 245\,5000.2092 + 0.07019 (17) \text{ E.} \quad (11)$$

The superhump excess is $\epsilon^+ = 0.0264$.

2.17 CSS1503-22 (CSS100216:150354-220711)

CSS1503-22, known as CSS100216:150354-220711, has a CSS light curve in which the star was at an average brightness $V \sim 19.9$ for about 5.5 years and then went into a high state with large excursions at an average $V \sim 17.5$. Our observations were made during the high state and are listed in Tab. 1. The light curves are shown in Fig. 31, phased on the 133.38 min period that we found in the FT. The existence of distinct window patterns at the first and third harmonics enables a unique choice among the aliases of the fundamental frequency. From its general optical behaviour we suspected this star to be a polar. We communicated the discovery to Julian Osborne at Leicester University and he confirmed from Swift X-Ray observations that it is indeed a

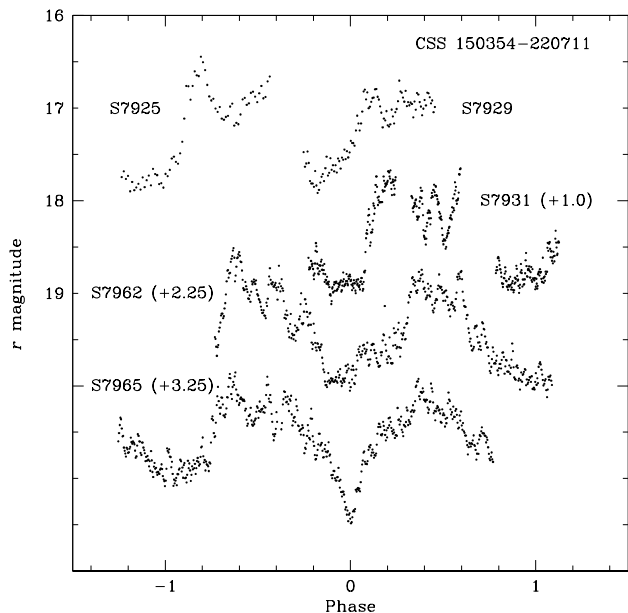


Figure 31. Individual light curves of CSS1503+22, folded on the ephemeris given in Eq. 12. The light curves of run S7925 and S7929 are displayed at the correct brightness. Runs S7931, S7962 and S7965 have been displaced vertically by 1, 2.25 and 3.25 mag, respectively.

magnetically accreting CV. Our ephemeris for the times of minimum light is

$$\text{HJD}_{\min} = 245\,5300.5757 + 0.092622 (15) \text{ E.} \quad (12)$$

2.18 CSS1528+03 (CSS090419:152858+034912)

CSS1528+03, or CSS 090419:152858+034912 in the CSS catalogue, is also in the Sloan survey second release (Szkody et al. 2003) as SDSS J1528+0349, where its spectrum shows it be a dwarf nova. Its CSS light curve shows variations from $V = 18.7$ to ~ 21 with rare outbursts to 17th magnitude. Our photometric observations, the first of which was taken during outburst, are listed in Tab. 1, and the two longest runs (both at quiescence) are shown as light curves in Fig. 32. There is strong flickering but no obvious modulation within our longest (~ 6 h) run. Either this CV has a very long orbital period or it is of low inclination.

2.19 CSS1626-12 (CSS090419:162620-125557)

CSS1626-12 is CSS090419:162620-125557 and has a CSS light curve which is undersampled but shows outbursts to $V \sim 17$ on time scales ~ 300 d. It is not detectable by CSS at quiescence, reaching $V > 20.4$. Our observations are listed in Tab. 1 and show that its un-eclipsed magnitude is in fact at $r = 20.4$. The average light curve is given in Fig. 33, where narrow eclipses to $r \sim 22.0$ are seen, recurring on the period $P_{orb} = 108.7$ min, with an ephemeris

$$\text{HJD}_{\min} = 245\,5352.4721 + 0.07546 (2) \text{ E.} \quad (13)$$

The light curve has a low amplitude orbital hump peaking at orbital phase 0.8 before being cut into by the eclipse.

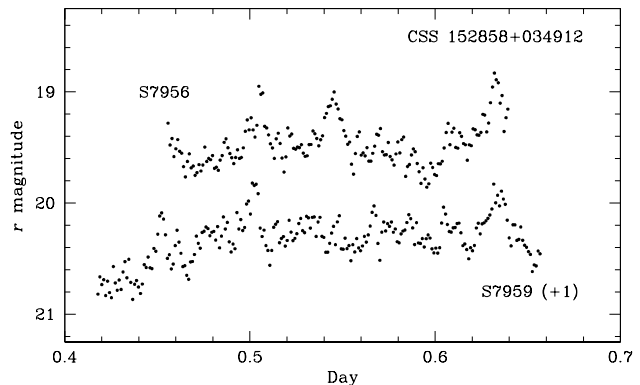


Figure 32. Individual light curves of CSS1528+03. The light curve of run S7956 is displayed at the correct brightness. Run S7959 has been displaced vertically by 1 mag for display purposes.

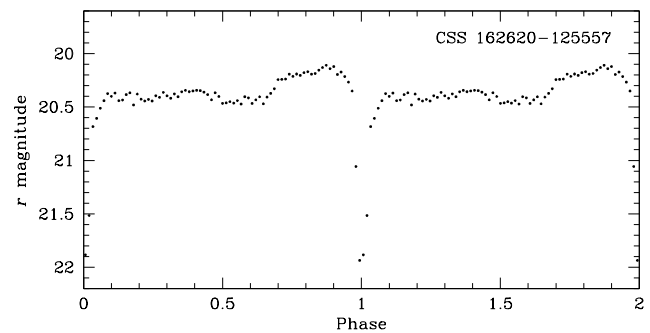


Figure 33. The average light curve of CSS1626-12, folded on the ephemeris given in Eq. 13.

2.20 EG Aqr (CSS080101:232519-081819)

CSS2325-08, or CSS 080101:232519-081819, is one of the first CVs to be found in the CSS survey and was a rediscovery of the known dwarf nova EG Aqr. Imada et al (2008) observed a superoutburst in EG Aqr in 2006 November and found a superhump period of 113.51 min. We observed EG Aqr at a quiescence brightness of $r \sim 19.3$ in 2008 October; the details are given in Tab. 1 and the light curves in Fig. 34. The FT of the combination of the best runs, S7817, S7819 and S7821, from consecutive nights is shown in Fig. 35.

In the FT there is only one pair of frequencies that are at a 2:1 ratio, which gives a period of 109.4 min and its first harmonic, which are indicated in Fig. 35 by the dashed vertical lines. We identify this with P_{orb} which gives a $\epsilon^+ = 0.0378$. The ephemeris for maximum light is:

$$\text{HJD}_{\max} = 245\,4757.2445 + 0.07596 (8) \text{ E.} \quad (14)$$

3 DISCUSSION

Our observations have assessed the properties of a further 20 faint CVs, resulting in the direct measurement of 15 orbital periods; the measurement of 2 further positive superhump periods with consequent determination of 3 fractional superhump excesses; and the measurement of two negative superhump periods. Among these are CSS 0322+02 which has both positive and negative superhumps in quiescence,

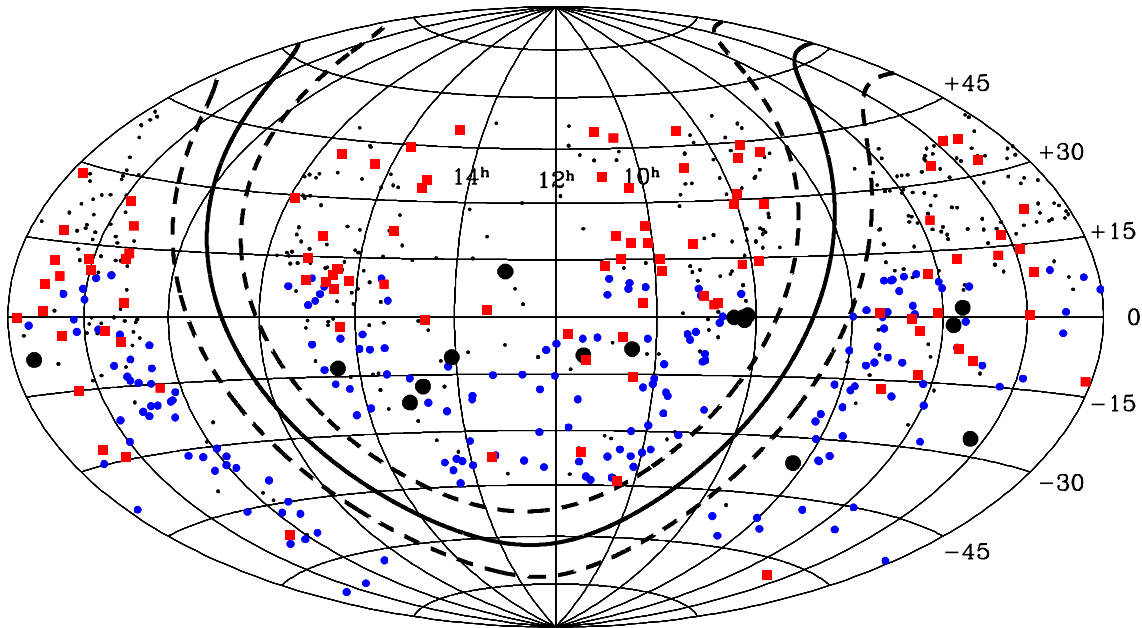


Figure 36. The distribution in an equatorial airtoff projection of CVs identified in the Catalina Real-Time Transient Survey. The Galactic Plane ($b = 0^\circ$) is marked by the solid line, the Galactic latitudes of $b = \pm 10^\circ$ are shown as dotted lines. The blue filled circles (colour is available only for the online version) mark those CVs observable from the SAAO with the 40-inch and 74-inch reflector and the UCT CCD (Declination (2000.0) $< +10^\circ$). Filled red triangles and squares display CVs with periods known prior to our photometric follow-up ($N = 100$), whereas the large black filled circles mark CVs with periods derived following the UCT CCD CV survey ($N = 15$).

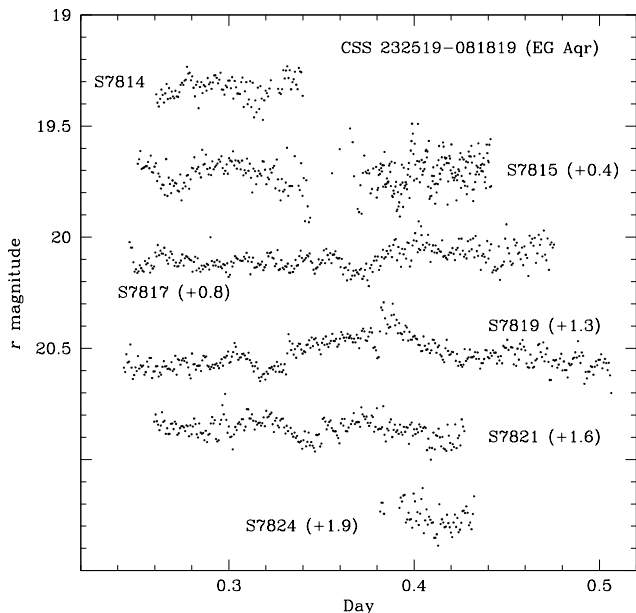


Figure 34. Individual light curves of CSS2325-08. The light curve of run S7814 is displayed at the correct brightness; vertical offsets for each light curve are given in brackets.

and CSS 0826-00, an eclipsing system with negative superhumps in quiescence, which potentially gives the possibility of deducing the brightness distribution of the negative superhump source.

CSS 0810+00 and CSS 1503-22 are new polars. SDSS 0919+08 has a known 260 s brightness modulation that

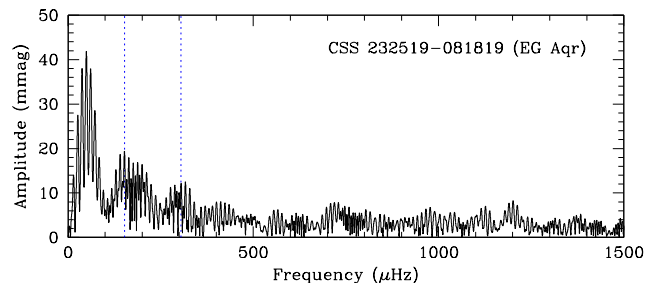


Figure 35. Fourier transform of the combined runs S7817, S7819 and S7821 of CSS2325-08.

could be interpreted either as non-radial pulsation or rotation; our discovery of an occasional additional 214 s periodicity points to the former explanation. CSS 0802+01 (HV Vir) had a previously suspected periodic signal near 120 min; we have observed a similar modulation, the origin of which is not known. A summary of the newly measured periods is included in Tab. 3.

Population syntheses combined with evolutionary computations of binary stars passing through the common envelope stage have long predicted that there should be a maximum space density of CVs near the minimum orbital period at $P_{orb} \sim 80$ min, which is where $dP_{orb}/dt = 0$ (e.g. Kolb & Baraffe 1999). But until recently this “period spike” had not been confirmed observationally. However, Gänsicke et al. (2009), from large numbers of faint CVs newly discovered in the SDSS survey, at last found evidence for the spike – because it occurs at small P_{orb} where the mass transfer rate is low the CVs have low accretion luminosity (typically $M_V \sim 11.5$), it is necessary to reach fainter than $V \sim 18$ be-

Table 3. Summary of results

Object	Type	P_{orb}^* (h)	P_{SH+}^\dagger (h)	P_{SH-} (h)	r	Remarks
SDSS0805+07	CV	5.489 (12)			17.9	
SDSS0904+03	CV	1.433358 (1)			19.2	Eclipsing
SSS0221-26	DN	1.692 (2)			19.3:	Possible alias at 1.818 h.
CSS0332+02	DN SU	1.469 (1)	1.5030 (2)	1.4387 (4)	20.2	Superhumps in quiescence
CSS0345-01	DN	1.684 (1)			18.6:	
SSS0617-36	CV	3.4404 (12)			17.7	
CSS0810+00	Polar	1.9358 (1)			18.2	High state
CSS0826-00	DN SU	1.4342 (2)		1.394 (1)	20.0	Eclipsing, superhumps in quiescence
CSS1028-08	DN	0.868 (10)	[0.914]		16.1-19.0	P_{SH+} from Kato et al. (2009)
CSS1300+11	DN SU	1.5041 (2)	[1.545]		19.8:	P_{SH+} from Kato et al. (2009)
CSS1404-10	DN SU	1.42990 (1)	1.464 (1)		16.6-19.6	Eclipsing, superhumps in outburst
CSS1443-17	DN	1.685 (4)	[1.7295]		19.1	P_{SH+} from Kato et al. (2009)
CSS1503-22	Polar	2.2229 (4)			17.2	High state
CSS1626-12	DN	1.811 (1)			20.4	Eclipsing
CSS2325-08	DN SU	1.823 (2)	[1.892]		19.3	P_{SH+} from Imada et al. (2008)

* Uncertainties are given between brackets for the last significant decimal(s). † Literature values are shown between square brackets.

fore the predicted population can be sampled. This was verified in another way by Wils et al. (2009) who cross-correlated a number of photometric and astrometric catalogues, finding 64 new CV candidates which, from the outburst amplitudes and frequencies of these and CRTS objects, imply that the CVs of faint apparent magnitudes are not simply more distant – there must also be a population of intrinsically faint systems. In affirmation, the CVs found in the Hamburg Quasar Survey, which have $B < 18.0$, fail to reveal the latter population (Aungwerojwit & Gänsicke 2009). Similarly, the CVs in the Calán-Tololo survey, which reaches down only to $B_J \sim 18.5$, have orbital periods that resemble those found in early surveys (Augusteijn et al. 2010).

The CRTS provides an independent source of faint CVs. Its requirement for a brightness range > 2 mag, together with its lower magnitude limit of $V \sim 20.5$, and the normal dwarf nova ranges of 2 – 5 mag and the rare SU UMA which range up to 8 mag, means that effectively quiescent magnitudes are sampled from $V \sim 20.5$ to 26, but they are probably biased towards the upper end of the luminosities as that is where the outburst frequency should be largest.

In Fig. 36 we show the on-sky distribution of all the ~ 640 CVs identified in the CRTS in an equatorial aiotoff projection; the CRTS avoids a zone of $\pm 10^\circ$ around the Galactic Plane and generally finds CVs between declinations of $+50^\circ$ and -70° . All CVs are shown as small (black) dots in this figure, with additional symbols for the 100 CVs that have measured superhump or orbital periods in the literature (red filled squares), those that are observable with the 40-in and 74-in reflectors from the Sutherland station of the SAAO (blue filled circles; declinations south of $+10^\circ$) and the 15 CVs with new periods determined in the course of the UCT CCD CV survey (black large filled circles).

We have generated a P_{orb} histogram using the CRTS source catalogue and all previous P_{orb} determinations (or P_s values, converted to P_{orb} with the Gänsicke et al. (2009) formula) supplemented with the new measurements from Tab. 3. Orbital periods are available for 115 of the ~ 650 known CRTS CVs, with 100 systems recorded in the literature (either in the Ritter & Kolb (2003) catalogue, or in

vsnet-alerts², where the latter predominantly report superhump periods) and an additional 15 orbital periods derived from the UCT CCD CV survey. Although the sample contains a small number of SDSS CVs that were already known before the CRTS survey began, it is almost independent and represents CVs found purely by the CRTS search technique. The result is shown in the lower panel of Fig. 37, where the SDSS distribution as found by Gänsicke et al. (2009) from 137 systems is also displayed (top panel). The CRTS histogram is similarly peaked but narrower than the SDSS histogram below the orbital period gap; overall both distributions reveal similar percentages of CVs in the 1.29 – 1.55 h period bins, namely 30% (CRTS) versus 32% (SDSS).

According to current understanding of the evolution of CVs those with P_{orb} between the minimum (bounce) period and ~ 2 h should be a mixture of pre- and post-bounce systems, the latter having degenerate secondaries and very low \dot{M} . Evidence for this is slowly increasing: Littlefair et al. (2008) have found three CVs where the secondaries are brown dwarfs, Patterson (2011) has given an extensive discussion and a list of possible candidates. This prediction is based on gravitational radiation (GR) being the driving mechanism for orbital evolution at short periods. Although that may be the only way that orbital angular momentum is lost on long time scales, it is clear that there is at least one other parameter that determines the present \dot{M} in CVs: the spread in absolute magnitudes of CVs below the orbital period gap (see, e.g., figure 12 of Warner 1987) shows that \dot{M} ranges over more than an order of magnitude, and the mean rate is several times that given by GR (Gänsicke et al. 2009). With the rapidly increasing number of known short period CVs it may become possible to investigate this more fully. We point out two relevant observational points:

The ER UMA stars lie at the high \dot{M} end of the range, they have superoutburst intervals, T_s , in the range 20 – 50 d and normal outburst intervals, T_n , ~ 5 d; only five members are currently known. They have the short orbital periods

² <http://ooruri.kusastro.kyoto-u.ac.jp/pipermail/vsnet-alert/>

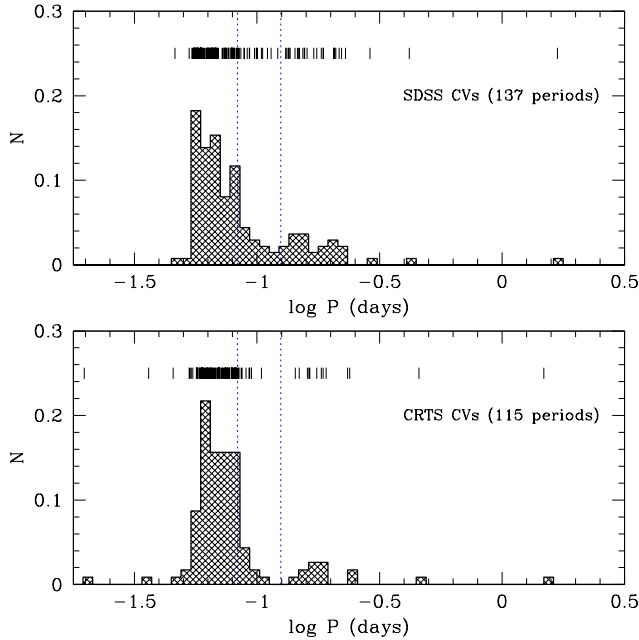


Figure 37. The period distribution of the 115 CRTS CVs (lower panel), compared to distribution of 137 SDSS CVs displayed in the upper panel (Gänsicke et al. (2009)). The distributions are normalised by the total number of CVs in each sample. The period gap is marked by the vertical dotted lines.

typical of SU UMa stars but appear isolated from the normal SU UMa stars by their short outburst intervals (Kato et al. 2003). They almost certainly must have exceptionally large \dot{M} (though additional parameters seem to be required - see discussion in Kato et al.); an analogy to the Z Cam stars at longer P_{orb} has been made (Warner 1995b). The few known ER UMa stars are probably only a small fraction of the true population - they are so variable that low cadence observations can fail to characterise them; indeed, the available CRTS light curves do not show their unusual outburst properties. The situation is similar to that of the earliest of them to be discovered, V1159 Ori, which was known as an irregular blue variable since 1906 but could not be appreciated fully until the 1990s. We expect that higher cadence and accepted amplitude range lowered to ~ 1 mag will provide many more examples, and perhaps fill the T_s gap between the ER UMa stars and the standard SU UMa stars.

More generally, we can use the CRTS light curves to segregate the dwarf novae into outburst classes. The light curves cover more than 5 years in a consistent way for all objects - they use all clear weather for 21 nights of each lunation and reach a cut-off magnitude ~ 20.5 . Although outbursts will be missed, the same fraction will be lost independent of frequency. We have simply assigned class 1 to light curves showing only one outburst, class 2 to two outbursts, and class 3 to > 2 outbursts. In the simplest interpretation these would correspond respectively to very low, low, and medium \dot{M} values.

The P_{orb} histograms of the three classes are shown in Fig. 38, excluding nine confirmed polars in the sample of 115 CRTS CVs with observed periods. There is a marked correlation between P_{orb} distribution and outburst class - in the sense that lower outburst frequencies are shifted towards

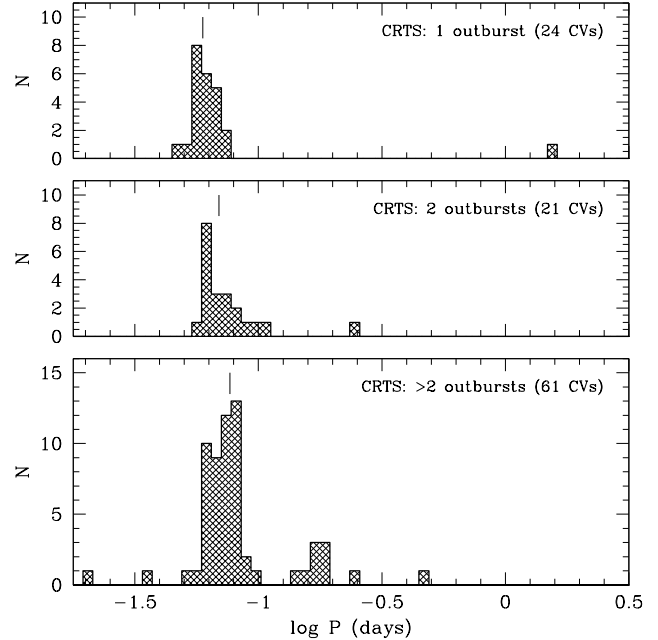


Figure 38. The period distribution of 106 CRTS dwarf novae: the top panel shows those with a single recorded outburst, the middle panel displays the dwarf novae with two outburst measured to date and the lower panel shows those with more than 2 outbursts in five years of CRTS observations. The median value of each period distribution is marked and corresponds to 1.43 h (top panel), 1.66 h (middle panel) and 1.82 h (lower panel), respectively. The ultra-compact helium-rich binaries with $P_{orb} \leq 65$ min and CVs with periods longer than 1 day were excluded from the median statistics.

shorter P_{orb} . But this trend should not arise from the simplest expected \dot{M} behaviour - if GR is operating alone then nearly constant \dot{M} is predicted (see equation 9.20 and figure 9.2 of Warner (1995a)) and the time taken to fill dwarf nova accretion discs between outbursts would be independent of P_{orb} . Other factors need to be taken into account, however - the space density of CVs per unit interval of P_{orb} is inversely proportional to the long term mean of \dot{M} (which would cancel with outburst frequency being directly proportional to \dot{M} to leave no P_{orb} dependence on average), but outburst frequency is determined for each system by its current \dot{M} - and as mentioned above this can be very different from the GR value and may depend on the past history of each system (e.g. when last it was a nova, in the hibernation scheme of things - see section 9.4.3 of Warner (1995a)).

A final conclusion is that the predictions of CV population studies are now beginning to be confirmed by observation - it required surveys reaching fainter than magnitude ~ 18.5 to detect the large population of highly evolved systems. Therefore the predicted end points of CV evolution should also be taken seriously - large numbers of cool Earth-sized white dwarfs with Jupiter-sized secondaries in ~ 2 h orbits, about 20% of which should show total eclipses.

ACKNOWLEDGMENTS

PAW and BW acknowledge support from the University of Cape Town (UCT) and from the National Research

Foundation of South Africa. PAW furthermore acknowledges financial support from the World University Network. DdB thanks the South African Square Kilometer Array project and UCT for financial support. SM received support from the National Astrophysics and Space Science Programme. We kindly thank Denise Dale for observations of SDSS0919+08. This paper uses observations made at the South African Astronomical Observatory (SAAO).

Woudt P.A., Warner B., Pretorius M.L., Dale, D., 2005, ASP Conf Ser 330, 325

REFERENCES

- Abazajian K.N., Adelman-McCarthy J.K., Agüeros M.A., et al., 2009, *ApJS*, 182, 543
- Augusteijn T., Tappert C., Dall T., Maza J., 2010, *MNRAS*, 405, 621
- Aungwerojwit A., Gänsicke B.T., 2009, ASP Conf. Ser. 404, 276
- Dillon M., Gänsicke B.T., Aungwerojwit A., et al., 2008, *MNRAS*, 386, 1568
- Drake A.J., Djorgovski S.G., Mahabal, A., et al., 2009, *ApJ*, 696, 870
- Gänsicke B.T., Dillon M., Southworth J., et al., 2009, *MNRAS*, 397, 2170
- Harvey D., Skillman D.R., Patterson J., Ringwald F.A., 1995, *PASP*, 107, 551
- Imada A., Stubbings R., Kato T., et al., 2008, *PASJ*, 60, 1151
- Jester S., Schneider D.P., Richards, G.T., et al., 2005, *AJ*, 130, 873
- Kato T., 2009, <http://ooruri.kusastro.kyoto-u.ac.jp/mailarchive/vsnet-alert/11028>
- Kato T., Bolt G., Nelson P., Monard B., Stubbings R., Pearce A., Yamaoka H., Richards T., 2003, *MNRAS*, 341, 901
- Kato T., Imada A., Uemura M., et al., 2009, *PASJ*, 61, S395
- Kolb U., Baraffe I., 1999, *MNRAS*, 309, 1034
- Landolt A., 1992, *AJ*, 104, 340
- Littlefair S.P., Dhillon V.S., Marsh T.R., Gänsicke B.T., Southworth J., Baraffe I., Watson C.A., Copperwheat C., 2008, *MNRAS*, 388, 1582
- Mukadam A.S., Gänsicke B.T., Szkody P., Aungwerojwit A., Howell S.B., Fraser O.J., Silvestri N.M., 2007, *ApJ*, 667, 433
- O'Donoghue D., 1995, *Baltic Ast*, 4, 517
- Olech A., Rutkowski A., Schwarzenberg-Czerny, A., 2007, *AcA*, 57, 331
- Olech A., Rutkowski A., Schwarzenberg-Czerny, A., 2009, *MNRAS*, 399, 465
- Patterson J., 2011, *MNRAS*, 411, 2695
- Patterson J., Thorstensen J.R., Kemp J., et al., 2003, *PASP*, 115, 1308
- Patterson J., Kemp J., Harvey D.A., et al., 2005, *PASP*, 117, 1204
- Ritter H., Kolb U., 2003, *A&A*, 404, 301 (update RKcat7.16, 2011)
- Sambruno R.M., Chiapetti L., Treves A., et al., 1991, *ApJ*, 374, 744
- Szkody P., Fraser O., Silvestri N., et al., 2003, *AJ*, 126, 1499
- Szkody P., Henden A., Fraser O.J., et al., 2004, *AJ*, 128, 1882
- Szkody P., Henden A., Fraser O.J., et al., 2005, *AJ*, 129, 2386
- Szkody P., Henden A., Mannikko L., et al., 2007, *AJ*, 134, 185
- Szkody P., Mukadam A., Gänsicke B.T., et al., 2010, *ApJ*, 710, 64
- Warner B., 1987, *MNRAS*, 227, 23
- Warner B., 1995a, *Cataclysmic Variable Stars*, Cambridge Univ. Press, Cambridge
- Warner B., 1995b, *Ap&SS*, 226, 187
- Warner B., 2004, *PASP*, 116, 115
- Wils P., Gänsicke B.T., Drake A.J., Southworth J., 2009, *MNRAS*, 402, 436
- Woudt P.A., Warner B., 2010, *MNRAS*, 403, 398